Development 120, 3033-3042 (1994)
Printed in Great Britain © The Company of Biologists Limited 1994

bcl-x$_L$ is the major *bcl-x* mRNA form expressed during murine development and its product localizes to mitochondria

Maribel González-García[1], Rafael Pérez-Ballestero[1], Liyun Ding[1], Linda Duan[1] Lawrence H. Boise[2], Craig B. Thompson[2] and Gabriel Núñez[1,*]

[1]Department of Pathology, University of Michigan Medical School, Ann Arbor, Michigan 48109, USA
[2]Howard Hughes Medical Institute, Departments of Medicine, Molecular Genetics and Cell Biology, University of Chicago, Chicago, Illinois 60637, USA

*Author for correspondence

SUMMARY

Most examples of cell death in animals are controlled by a genetic program that is activated within the dying cell. The apoptotic process is further regulated by a set of genes that act as repressors of cell death. Of these, *bcl-2* is expressed in a variety of embryonic and postnatal tissues which suggests a critical role for *bcl-2* in organogenesis and tissue homeostasis. Surprisingly, mutant mice with targeted disruption of *bcl-2* appear normal at birth and complete maturation of lymphoid tissues before succumbing to fulminant lymphopenia and polycystic renal disease by 2-5 weeks of age. This suggests that there may be genes other than *bcl-2* that can regulate apoptosis during development. To begin to investigate this possibility, we have cloned and characterized the murine *bcl-x* gene, whose human counterpart displays striking homology to *bcl-2*. The predicted murine *bcl-x*$_L$ gene product exhibits a high level of amino acid identity (97%) to its human counterpart. Just like Bcl-2, the murine *bcl-x*$_L$ gene product can act as a dominant inhibitor of cell death upon growth factor withdrawal. In addition, the bulk of the *bcl-x*$_L$ product localizes to the periphery of mitochondria as assessed by a *bcl-x*$_L$-tag expression system, suggesting that both Bcl-2 and Bcl-x$_L$ proteins prevent cell death by a similar mechanism. *bcl-x*$_L$ is the most abundant *bcl-x* mRNA species expressed in embryonic and adult tissues. The levels of *bcl-x*$_L$ mRNA appear higher than those of *bcl-2* during embryonal development and in several adult organs including bone marrow, brain, kidney and thymus. In addition to *bcl-x*$_L$, we have identified another form of *bcl-x* mRNA, *bcl-x*$_\beta$, that results from an unspliced *bcl-x* transcript. *bcl-x*$_\beta$ mRNA is expressed in various embryonic and postnatal tissues. Surprisingly, the expression of *bcl-x*$_S$ (a negative regulator of programmed cell death) was undetectable by a sensitive S1-nuclease assay and polymerase chain reaction analysis of mouse tissues. Based on its tissue and developmental patterns of expression, it appears that *bcl-x* may play an important role in the regulation of cell death during development and tissue homeostasis.

Key words: Apoptosis, *bcl-x*, *bcl-2*, cell death

INTRODUCTION

Cellular homeostasis and development in vertebrates is regulated by several processes that include cell proliferation, differentiation and cell death. The death of cells can be conceptually divided into two main categories: accidental cell death (necrosis) and naturally occurring cell death or Programmed Cell Death (PCD) that is often accomplished by apoptosis. PCD is widespread during embryogenesis, endocrine-dependent cellular atrophy, normal cellular turnover, and clonal selection in the immune system (Ellis et al., 1991). For example, during development of the central nervous system in vertebrates, as much as 85% of certain populations of neurons undergo cell death (reviewed by Oppenheim, 1991). The death mechanism appears to occur through competition for trophic factors derived from target tissues, which may serve to select the proper set of neuronal connections (Oppenheim, 1991). Similarly, in postnatal tissues, terminal differentiation of complex epithelia such as that from the skin is coupled to PCD (McCall and Cohen, 1991). In the immune system, PCD plays a critical role in the selection of appropiate lymphoid populations (Cohen, 1991). Thus, PCD plays an important role during development and tissue turnover by reinforcing appropriate cellular patterns or removing cells that are harmful or no longer needed.

PCD appears to be a genetically regulated process. PCD can be induced by a variety of stimuli, including deprivation of essential growth factors, signalling via certain cell surface receptors or exposure to hormones or drugs such as corticosteriods (Ellis et al., 1991; Williams, 1991). Although the mechanisms of PCD are poorly understood, it is generally thought that dying cells participate in their own demise by activating a genetically programmed suicide pathway (Cohen and Duke, 1984; Martin et al., 1988). In the nematode *Caenorhabditis elegans*, fourteen genes have been identified that are involved in the death of somatic cells during development (reviewed by

Ellis et al., 1991). Some of these genes act at an early stage of the pathway, whereas other genes are directly responsible for the cell death mechanism. For example, mutations that inactivate two autosomal recessive genes *ced-3* and *ced-4*, prevented normal patterns of cell death during development (Ellis and Horvitz, 1986). The *ced-3* and *ced-4* genes encode proteins that may display killing activity themselves or regulate such activity in cells (Yuan and Horvitz, 1990; Yuan et al., 1993). In contrast to *ced-3* and *ced-4*, *ced-9* acts by suppressing cell death. Inactivation of *ced-9* by mutation causes death in many different cells during *C. elegans* development (Hengartner et al., 1992). Similarly, genes that control the cell death pathway in the developing eye of *Drosophila melanogaster* have been identified recently (Bonini et al., 1993).

In mammals, several genes have been isolated recently that are induced upon activation of the PCD pathway (Baughman et al., 1991; Owens et al., 1991; Ishida et al., 1992). Wild-type p53 has been shown to induce apoptosis (Yonish-Rouach et al., 1991; Ryan et al., 1993) and appears to be required for several forms of PCD (Lowe et al., 1993; Clarke et al., 1993). In addition, overexpression of the *ced-3* homolog, interleukin-1β-converting enzyme, can directly activate PCD (Miura et al., 1993). Two related mammalian genes, *bcl-2* and *bcl-x* have been identified that function as suppressors of PCD. *bcl-2* was discovered at the breakpoint region of a recurrent chromosomal translocation t(14;18) (q32;q21) identified in up to 85% of follicular B-cell lymphomas (Tsujimoto and Croce, 1986). The product of *bcl-2* is a 26×10^{-3} M_r integral-membrane protein that has been localized to mitochondria, perinuclear membrane, and smooth endoplasmic reticulum (Hockenbery et al., 1990; Monaghan et al., 1992; Jacobson et al., 1993; Krajewski et al., 1993). Several studies have shown that overexpression of Bcl-2 can prevent many forms of PCD (Vaux et al., 1988; Núñez et al., 1990; García et al., 1992). *bcl-x* was identified in the chicken by hybridization with a murine *bcl-2* probe (Boise et al., 1993). Subsequently, two distinct *bcl-x* cDNAs, *bcl-x*$_L$ and *bcl-x*$_S$, were isolated in the human. The predicted Bcl-x$_L$ protein displays remarkable amino acid and structural homology to Bcl-2. Transfection of *bcl-x*$_L$ into IL-3-dependent cells prevented their apoptotic cell death following growth factor deprivation. The predicted Bcl-x$_S$ protein differs from Bcl-x$_L$ in that an internal region of 63 amino acids displaying the greatest homology to Bcl-2 has been deleted by alternative splicing of the primary *bcl-x* mRNA transcript. Importantly, expression of *bcl-x*$_S$ failed to inhibit cell death but it facilitated the apoptotic process by inhibiting the death suppressor activity of Bcl-2 (Boise et al., 1993).

Initial analysis revealed that *bcl-x* was expressed in a variety of tissues in the chicken. Furthermore, the expression of *bcl-x*$_L$ and *bcl-x*$_S$ appeared differentially regulated in human tissues as determined by the polymerase chain reaction (PCR). For example, *bcl-x*$_L$ mRNA but not *bcl-x*$_S$ mRNA was detected in adult human brain (Boise et al., 1993). These preliminary studies suggested that *bcl-x*$_L$ and *bcl-x*$_S$ may play distinct functional roles during development. In order to assess in more detail the developmental role of *bcl-x* in the animal, we have isolated the murine *bcl-x* homolog. Murine Bcl-x$_L$ is a non-nuclear intracellular protein that, like Bcl-2, localizes to the mitochondria and perinuclear envelope and can prevent cell death induced by growth withdrawal in murine tissue culture cells. These data suggest that both Bcl-2 and Bcl-x$_L$ may function by a similar mechanism to inhibit cell death. Our results show that *bcl-x*$_L$ is the dominant species of *bcl-x* mRNA expressed in murine tissues during embryonic and postnatal development. Importantly, *bcl-x*$_S$ is undetectable in the embryo and adult organs arguing against a role of *bcl-x*$_S$ in tissue development. However, a novel form of *bcl-x* mRNA, *bcl-x*$_\beta$, which results from an unspliced mRNA transcript is expressed in embryonal and postnatal tissues. A truncated *bcl-2* gene construct similar to *bcl-x*$_\beta$, appears capable of at least partially inhibiting apoptosis (Hockenbery et al. 1993). Together, these data suggest that in addition to *bcl-2*, *bcl-x*$_L$ will have an important role in the regulation of developmental cell death and tissue homeostasis.

MATERIAL AND METHODS

Cloning and construction of plasmids

A murine brain cDNA library cloned into the Uni-ZAP XR vector (Stratagene) was screened with a human *bcl-x* probe (Boise et al., 1993). Filter hybridization was performed in 50% formamide, 6× SSPE, 5× Denhardt's solution, 0.5% SDS and 100 μg/ml denatured salmon sperm DNA at 37°C overnight. The final washing conditions were in 2× SSPE at 37°C three times. Inserts from positive clones were sequenced by a dideoxy termination method. Genomic *bcl-x* clones were isolated from a murine liver library (a gift of Dr Paul Killen, University of Michigan) by hybridization with a full-lengh murine *bcl-x*$_L$ cDNA. Analysis of genomic clones was performed by restriction mapping, hybridization with oligonucleotide probes complementary to different regions of the *bcl-x*$_L$ cDNA and sequencing. The murine *bcl-x*$_\beta$ cDNA was isolated from a murine thymic cDNA library constructed in λZAP (Stratagene) by PCR amplification using primers corresponding to sequences in the *bcl-x* coding region (5′-CTAGAATTCAAATGTCTCAGAGCAACCG-3′) and in the second intron of *bcl-x* (5′-CCAGAATTCAGGCCTGAACAATCG-GTATCT-3′). A band of appropriate size (0.8 kb) was subcloned into pBluescript and inserts were sequenced. To generate a 8 amino acid FLAG tag that contains a well-characterized epitope (Hopp et al., 1988), FLAG sequences were attached to the N-terminus of the murine Bcl-x$_L$ protein by PCR. The 5′ primer (5′-AGAGAATTCC-CACCATGGACTACAAGGACGACGATGACAAGTCTCAGAG-CAACCGG-3′) incorporated a FLAG tag to Bcl-x$_L$ and a consensus translation site (Kozak, 1986). The 3′ primer (5′-TGGGAATTCAGT-GTCTGGTCACTTCCG-3′) contained the natural *bcl-x*$_L$ stop codon. Both primers included Eco RI linkers to facilitate subcloning. Amplification of FLAG-*bcl-x*$_L$ was performed by PCR through 35 cycles (1 minute at 94ºC, 1 minute at 56°C, 1 minute at 72°C). The authenticity of FLAG-*bcl-x*$_L$ was confirmed by sequencing. The insert was excised from a low melting agarose gel, digested with *Eco*RI and subcloned into the expression vector pSFFV-Neo (Fuhlbrigge, 1988). Orientation of the inserts was determined by restriction enzyme mapping. The plasmid with the murine FLAG-*bcl-x*$_L$ insert in the forward orientation was designated FLAG-m*bcl-x*$_L$ and the plasmid with FLAG-m*bcl-x*$_L$ in reversed orientation, FLAG-*mbcl-x*$_L$-rev. Sequence comparison and peptide analysis was performed with the University of Wisconsin Genetics Computer Group programs.

Cell transfection and functional analysis

Murine FL5.12 cells were cultured as previously described (Núñez et al., 1990). Cells were transfected by electroporation (200 V, 960 μF) with 15 μg of plasmid DNA. Transfectants were selected by growth in the presence of G418 (1 mg/ml). Cell survival before and after IL-3 deprivation was assessed as previously described (Núñez et al., 1990). Expression of the FLAG-Bcl-x$_L$ protein was determined by

flow cytometry as previously described (Boise et al., 1993). The FLAG epitope was detected using M2, a mouse anti-FLAG monoclonal antibody (International Biotechnologies). As a control, cells were stained with a murine monoclonal antibody directed to the 12CA5 influenza virus hemaglutinin protein epitope (Kolodziej and Young, 1991).

RNA preparation and northern blot analysis

Embryonal tissue was isolated from CD-1 mice (first day was taken as the day of vaginal plug appearance). Adult organs were prepared from 8- to 20-week old C57BL/6 mice (Jackson Laboratories). Total mRNA was isolated from mouse tissues by the guanidinium isothiocyanate method followed by cesium chloride gradient centrifugation (Chirgwin et al., 1987). For northern analysis, 12 μg of total mRNA was separated on agarose-formaldehyde gels, blotted onto nitrocellulose filters and hybridized overnight with ^{32}P-labeled probes. The final washing conditions were 0.1% SSC, 0.1% SDS at 56°C for 20 minutes. Blots were stripped by boiling.

S1 nuclease protection assay

The generation of the murine *bcl-2* probe has been described previously (Cuende et al., 1993). The 5′ end of the antisense strand was labeled at the *Bam*HI site located in the coding region of *bcl-2* using [^{32}P]ATP (6,000 Ci/mmol) (Amersham) as described (Cuende et al., 1993). To construct a murine *bcl-x* probe, a 725 bp cDNA fragment containing the entire coding region of *bcl-x$_L$* was inserted into the *Eco*RI polylinker site of pBluescript. The 3′ end of the antisense strand was labeled at the unique *Sal*I site of *bcl-x$_L$* by filling with [^{32}P]dCTP (6,000 Ci/mmol) (Amersham) and Klenow (Promega) (see Fig. 4A). To assess mRNA expression, equal amounts of *bcl-2* and *bcl-x* labeled probes (10^5 cpm each) were hybridized simultaneously with total mRNA samples in the same tube for 16 hours at 55°C and then digested with 200 U of S1 nuclease for 1 hour at 37°C. Protected fragments were size separated on a 6% sequencing gel, dried, and autoradiographed. Autoradiographs were quantified by densitometry scanning with a Radioanalytic Imaging system and AMBIS Quant-Probe Software (AMBIS, Inc., San Diego, CA.)

Laser-scanning microscopy

Cells were washed in PBS, adhered to polylysine-coated slides, fixed with 2% paraformaldehyde for 10 minutes and then permeabilized with 0.1% saponin (Sigma) for 15 minutes at 23°C. After washing in PBS containing 0.03% saponin, the cells were blocked with 20% normal goat serum and labeled with M2, a mouse anti-FLAG monoclonal antibody or control mouse anti-12AC5 epitope mAb (Kolodziej and Young, 1991) for 45 minutes at 23°C. The reaction was visualized with fluorescein-coupled to goat anti-mouse IgG (BRL). For double-labeling analysis, cells were first incubated with 100 nM of the dye MitoTracker (mitochondria marker) or 5 μM of CellTracker (cytosol marker) (both from Molecular Probes, Eugene, Oregon), for 20 minutes at 37°C, washed, and fixed with 2% paraformaldehyde as above. Cells were then permeabilized with 0.1% saponin and incubated with mouse anti-FLAG monoclonal antibody as described above. Control cells were stained with either dye or anti-FLAG alone. After staining, the cells were mounted in Slowfade (Molecular Probes) and examined using a BioRad MRC 600 scanning confocal microscope equipped with an argon-xenon laser and K1/K2 filters for dual labeling analysis.

Electron microscopy

Cells were fixed in 2% paraformaldehyde and 0.01% glutaraldehyde for 15 minutes at 4°C, washed in PBS and permeabilized with 0.1% saponin for 10 minutes. Cells were preincubated with 20% normal goat serum and incubated with M2 (anti-FLAG) or control anti-12AC5 murine monoclonal antibodies for 45 minutes at 23°C. After washing in PBS, cells were incubated with biotinylated goat anti-mouse IgG (Vector Laboratories) for 30 minutes at 23°C and HRPase-avidin-biotin complex reagent (ABC kit, Vector Laboratories). Following two washes in PBS, the reaction was developed with 0.5 mg/ml of diaminobenzidine (DAB) and 0.01% H_20_2 for 5 minutes. After washing with PBS, the cells were fixed with 2% glutaraldehyde for 10 minutes, and postfixed with 1% OsO_4 in rinse buffer (0.1 M sodium cacodylate, 0.12 M sucrose and 2 mM $CaCl_2$, pH 7.4). Following washing in rinse buffer, cells were dehydrated by sucessive incubations in graded solutions of ethanol. Preembedding was performed in a 50% mixture of propylene oxide and Epon 812 (v/v) at 23°C for 2 hours. Cells were then embedded in Epon 812 resin at 23°C and the reaction polymerized at 60°C overnight. Ultrathin sections (70-90 nm) were mounted on mesh copper grids. Analysis was performed using a Phillips CM-10 electron microscope (Phillips Electronic Instruments).

RESULTS

Isolation and sequence analysis of the murine *bcl-x* cDNA

To isolate the murine *bcl-x* homolog, a cDNA library from adult murine brain was screened with a human *bcl-x* probe. Eight positive phages were isolated with inserts ranging from 1.3 to 2.7 kb. All cDNAs contained identical overlapping sequences as assessed by restriction endonuclease mapping and sequencing analysis. The longest cDNA contained an open reading frame of 233 amino acids with high level nucleotide sequence identity (93%) to the *bcl-x$_L$* form of human *bcl-x* (Fig. 1). None of the cDNAs isolated from the mouse brain library represented the murine counterpart of human *bcl-x$_S$* (Boise et al., 1993). These results established that the cDNA isolated from brain tissue is the murine homolog of *bcl-x$_L$*. Further comparative analysis revealed that the predicted coding region of murine *bcl-x$_L$* displayed 97% amino acid identity to human Bcl-x$_L$ and 44% identity to mouse Bcl-2 (Fig. 2). The homology between Bcl-x$_L$ and Bcl-2 extended over the entire coding region but it was particularly striking in an internal stretch of 63 amino acids, which is absent in the predicted human Bcl-x$_S$ protein (Boise et al. 1993; Fig. 2). In addition, there were stretches of high identity between Bcl-x$_L$ and Bcl-2 at the N-terminal region (Fig. 2). Both human and murine Bcl-x$_L$ proteins contained a C-terminal domain of 19 amino acids flanked by charged residues (Boise et al., 1993; Fig. 2). This hydrophobic amino acid stretch is typical of a membrane-spanning region and has been shown to serve as an anchoring domain for Bcl-2 (Chen-Levy et al., 1989; Hockenbery et al., 1990; Nguyen et al., 1993).

Bcl-x$_L$ is a non-nuclear intracytoplasmic protein that localizes to mitochondria

The Bcl-2 protein localizes to membranes of the mitochondria, and to a lesser extent, to the perinuclear space and smooth endoplasmic reticulum and can protect cells from various forms of cell death (Hockenbery et al., 1990; Monaghan et al., 1992; Jacobson et al., 1993; Krajewski et al., 1993). Because antibodies specific for Bcl-x are not yet available, we constructed a plasmid to express an 8-amino-acid tag peptide (FLAG) fused to the N terminus of the murine Bcl-x$_L$ protein to assess its subcellular localization. Stable transfection of the FLAG-*bcl-x$_L$* gene into murine FL5.12 cells resulted in high expression of the Bcl-x$_L$ protein as determined by flow cytometric analysis (Fig.

3A). Importantly, both the murine FLAG-Bcl-x_L and wild-type Bcl-x_L proteins inhibited the apoptotic death of FL5.12 cells deprived of IL-3 (Fig. 3B). This demonstrates that murine Bcl-x_L can function to inhibit cell death induced by growth factor withdrawal and that the 8-amino acid FLAG tag does not alter its biological function. Analysis of labeled cells with anti-FLAG monoclonal antibody revealed that Bcl-x_L displays an intracellular location as determined by laser scanning confocal microscopy (Fig. 3C). The labeling pattern was granular and extranuclear similar to that observed for Bcl-2 (Hockenbery et al., 1990; Jacobson et al., 1993; Krajewski et al., 1993), consistent with a localization of Bcl-x_L within intracytoplasmic organelles. Dual labeling experiments showed that the staining with fluorescein-labeled FLAG-Bcl-x_L is coincident with the distribution of MitoTracker, a rhodamine dye that targets to the mitochondria (Fig. 4A,B). The staining pattern of fluorescein FLAG-Bcl-x_L was different from that observed with CellTracker, a dye that accumulates in the cytosolic compartment and exhibits a diffuse non-granular staining pattern (Fig. 4C,D). To further define its subcellular distribution, we performed immunoelectron microscopic studies of FL5.12 cells expressing FLAG-Bcl-x_L. The analysis revealed that the bulk of the FLAG-Bcl-x_L protein localizes to the periphery of mitochondria (Fig. 5A). Within the lymphoid FL5.12 cells, which contain abundant mitochondria, the distribution pattern of FLAG-Bcl-x_L complexes within individual mitochondria was non-uniform and patchy (Fig. 5A). In addition, focal distribution of FLAG-Bcl-x_L was present on the nuclear envelope (Fig. 5A). No labeling was identified in the nucleus or plasma membrane. The staining was specific in that no immunostaining was observed when untransfected FL5.12 cells were stained with anti-FLAG antibody (Fig. 5B) or FLAG-bcl-x_L transfected cells were labeled with an isotype-matched control monoclonal antibody (data not shown). Thus, the subcellular distribution of Bcl-x_L is similar to that reported for Bcl-2 (Monaghan et al., 1992; Jacobson et al., 1993; Krajewski et al., 1993).

Expression of *bcl-x* mRNA in murine tissues

To characterize *bcl-x* further, its expression pattern was assessed in mouse tissues. Northern blot analysis revealed an approx. 3 kb mRNA species present in all tissues examined. Highest levels of *bcl-x* expression were found in the brain, thymus, bone marrow and kidney (Fig. 6). In the human, two different *bcl-x* mRNA species, *bcl-*x_L and *bcl-*x_S, have been identified by cDNA cloning and PCR analysis (Boise et al., 1993). To assess the expression of *bcl-x* forms in mouse tissues, a quantitative S1-nuclease assay was developed to discriminate between *bcl-*x_L and *bcl-*x_S forms (Fig. 7A). The assay included hybridization of mRNAs to both end-labeled *bcl-x* and *bcl-2* S1-nuclease probes to allow assessment of the relative abundance of *bcl-2* and *bcl-x* mRNAs. Results shown in Fig. 7B revealed that *bcl-*x_L is the predominant mRNA expressed in postnatal tissues. *bcl-*x_L was more abundant (2- to 6-fold) than *bcl-2* in all adult tissues evaluated, except in lymph nodes. The greater abundance of *bcl-*x_L over *bcl-2* was particularly evident in adult brain, thymus, and kidney (5- to 6-fold). In the whole embryo, *bcl-*x_L mRNA was detected at day 8.5 through 12.5 of development and was expressed at day 15.5 in several tissues examined including liver, heart, brain, and kidney (Fig. 7C). *bcl-*x_L was particularly abundant in embryonic liver, the major site of hematopoiesis in the embryo, which is consistent with its elevated expression in adult bone marrow and thymus. Surprisingly, no *bcl-*x_S mRNA species were detected in embryonal and adult tissues including the thymus where it was previously detected in the human by PCR analysis (Boise et al., 1993; Fig. 7B,C). The failure to

```
gaattcggcacgagtttttttttttttctgagttaccggcgacccagccaccacctcctccccg    65

acctatgattcaaaagaccttccgggggttgtacctgcttgctggtcgccggagatagatttgaa   130

taacttatcttggctttggatcctggaagagaatcgctaaacacagagcagacccagtaagtgag   195

caggtgttttggacaatggactggttgagcccatctctattataaaa atg tct cag agc     254
                                                  M   S   Q   S

aac cgg gag ctg gtg gtc gac ttt ctc tcc tac aag ctt tcc cag aaa      302
 N   R   E   L   V   V   D   F   L   S   Y   K   L   S   Q   K

gga tac agc tgg agt cag ttt agt gat gtc gaa gag aat agg act gag      350
 G   Y   S   W   S   Q   F   S   D   V   E   E   N   R   T   E

gcc cca gaa gaa act gaa gca gag agg gag acc ccc agt gcc atc aat      398
 A   P   E   E   T   E   A   E   R   E   T   P   S   A   I   N

ggc aac cca tcc tgg cac ctg gcg gat agc ccg gcc gtg aat gga gcc      446
 G   N   P   S   W   H   L   A   D   S   P   A   V   N   G   A

act ggc cac agc agc agt ttg gat gcg cgg gag gtg att ccc atg gca      494
 T   G   H   S   S   S   L   D   A   R   E   V   I   P   M   A

gca gtg aag caa gcg ctg aga gag gca ggc gat gag ttt gaa ctg cgg      542
 A   V   K   Q   A   L   R   E   A   G   D   E   F   E   L   R

tac cgg aga gcg ttc agt gat cta aca tcc cag ctt cac ata acc cca      590
 Y   R   R   A   F   S   D   L   T   S   Q   L   H   I   T   P

ggg acc gcg tat cag agc ttt gag cag gta gtg aat gaa ctc ttt cgg      638
 G   T   A   Y   Q   S   F   E   Q   V   V   N   E   L   F   R

gat gga gta aac tgg ggt cgc atc gtg gcc ttt ttc tcc ttt ggc ggg      686
 D   G   V   N   W   G   R   I   V   A   F   F   S   F   G   G

gca ctg tgc gtg gaa agc gta gac aag gag atg cag gta ttg gtg agt      734
 A   L   C   V   E   S   V   D   K   E   M   Q   V   L   V   S

cgg att gca agt tgg atg gcc acc tat ctg aat gac cac cta gag cct      782
 R   I   A   S   W   M   A   T   Y   L   N   D   H   L   E   P

tgg atc cag gag aac ggc ggc tgg gac act ttt gtg gat ctc tac ggg      830
 W   I   Q   E   N   G   G   W   D   T   F   V   D   L   Y   G

aac aat gca gca gcc gag agc cgg aaa ggc cag gag cgc ttc aac cgc      878
 N   N   A   A   A   E   S   R   K   G   Q   E   R   F   N   R

tgg ttc ctg acg ggc atg act gtg gct ggt gtg gtt ctg ctg ggc tca      926
 W   F   L   T   G   M   T   V   A   G   V   V   L   L   G   S

ctc ttc agt cgg aag tga ccagacactgaccgtccactcacctctcacctccc         979
 L   F   S   R   K   *
```

Fig. 1. Nucleotide sequence and predicted open reading frame of mouse *bcl-x*. The sequence was derived from a cDNA isolated from mouse brain. The predicted stop codon is indicated by an asterisk. Comparison analysis revealed that the murine and human *bcl-*x_L open reading frames (Boise et al., 1993) were 93% identical at the nucleotide level.

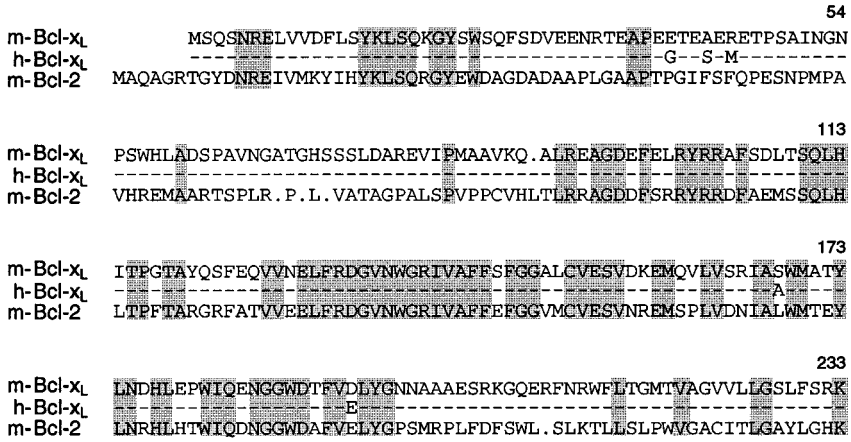

Fig. 2. Comparison of the Predicted Human and Murine Bcl-x_L/Bcl-2 Proteins. The alignment was maximized by introducing insertions marked by dots. Areas of amino acid identity between m (murine) and h (human) Bcl-x_L proteins are indicated by a dash. Areas of amino acid identity between Bcl-2 and Bcl-x_L proteins are marked by stippling.

detect murine *bcl-x$_S$* was confirmed using three additional S1-probes that were end-labeled at different sites of the 5′ and 3′ ends of the *bcl-x* coding region. Furthermore, *bcl-x$_S$* was also undetectable by a more sensitive PCR assay, and in tissues from two additional inbred mouse strains ruling out the possibility that the results were due to differences in genetic background (data not shown). Interestingly, a form of *bcl-x* mRNA, *bcl-x$_\beta$*, distinct from *bcl-x$_L$* and *bcl-x$_S$* was readily identified in mouse embryonal and posnatal tissues by S1-nuclease analysis (Fig. 7B,C). The size of the protected band identified by S1 mapping predicted that *bcl-x$_\beta$* and *bcl-x$_L$* sequences overlap at the 5′ end but differ at the 3′ region of *bcl-x* (Fig. 7A).

The *bcl-x$_\beta$* form lacks a hydrophobic C-terminal domain and derives from an unspliced *bcl-x* mRNA transcript

To analyse in more detail *bcl-x$_\beta$*, genomic clones of the murine *bcl-x* gene were isolated and characterized by restriction endonuclease mapping and sequence analysis. These studies revealed that *bcl-x$_\beta$* arose from an unspliced mRNA, since it is colinear with the genomic sequences (Fig. 8A). Sequence analysis of the *bcl-x$_\beta$* cDNA isolated revealed an open reading frame of 209 amino acids long, of which the first 188 residues overlap with Bcl-x_L including an internal region with high homology to Bcl-2 (Fig. 8B). When compared to Bcl-2, Bcl-xβ displayed the highest amino acid homology to the Bcl-2β product of *bcl-2* (Negrini et al., 1987). Both Bcl-2β and Bcl-xβ proteins lack a stretch of 19 hydrophobic amino acids at the C terminus flanked by charged residues, which is present in

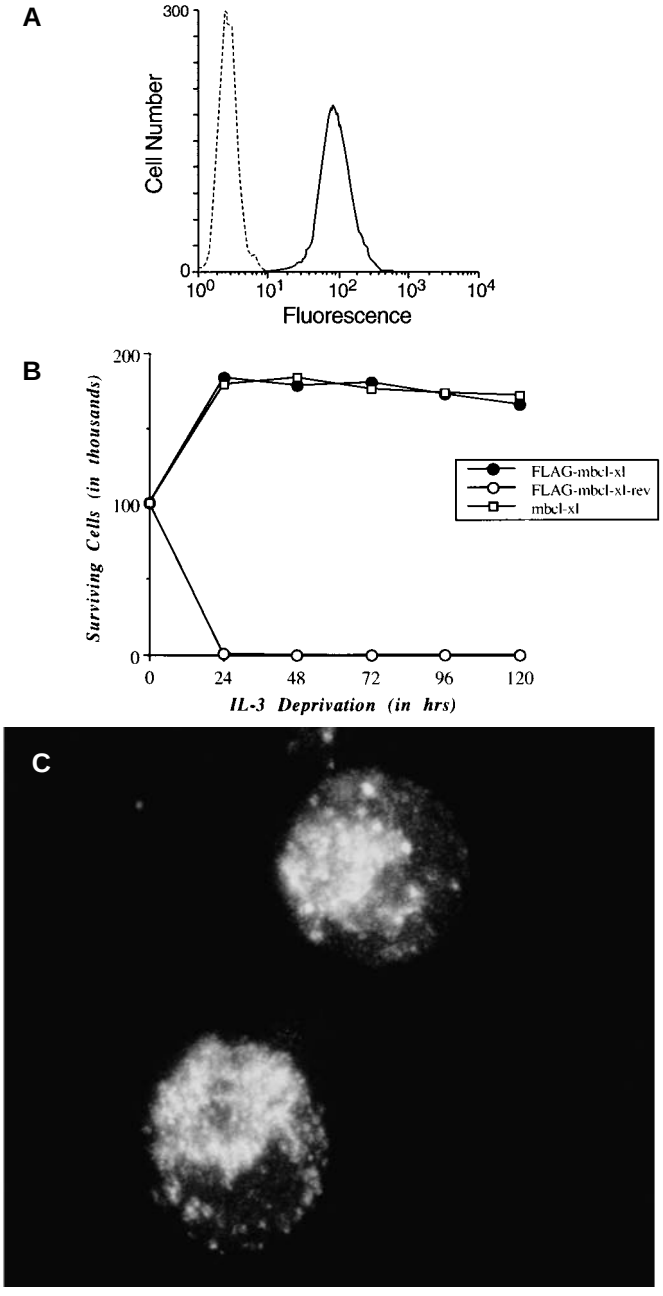

Fig. 3. Expression and fluorescence localization of FLAG-Bcl-x_L in FL5.12 cells. (A) Stably transfected FLAG-bcl-x_L cells were permeabilized and stained with anti-FLAG (solid line) or control antibody (dotted line) as described in Materials and Methods. (B) Survival of stable transfectants of FL5.12-expressing FLAG-m*bcl-x$_L$* (closed circles), wild-type *mbcl-x$_L$* (open squares) or FLAG-*mbcl-x$_L$*-rev (open circles) following IL-3 deprivation. Cell survival was determined as previously described (Núñez et al., 1990). Results are expressed as the mean of triplicate cultures. Standard deviation was less than 10% of the mean value. (C) Confocal images of FL5.12 cells transfected with FLAG-*bcl-x$_L$*. Cells were stained and analyzed as described in Materials and Methods. Control cells stained with irrelevant murine monoclonal antibody or parental cells labeled with anti-FLAG antibody were unstained (data not shown). Magnification 4,000×.

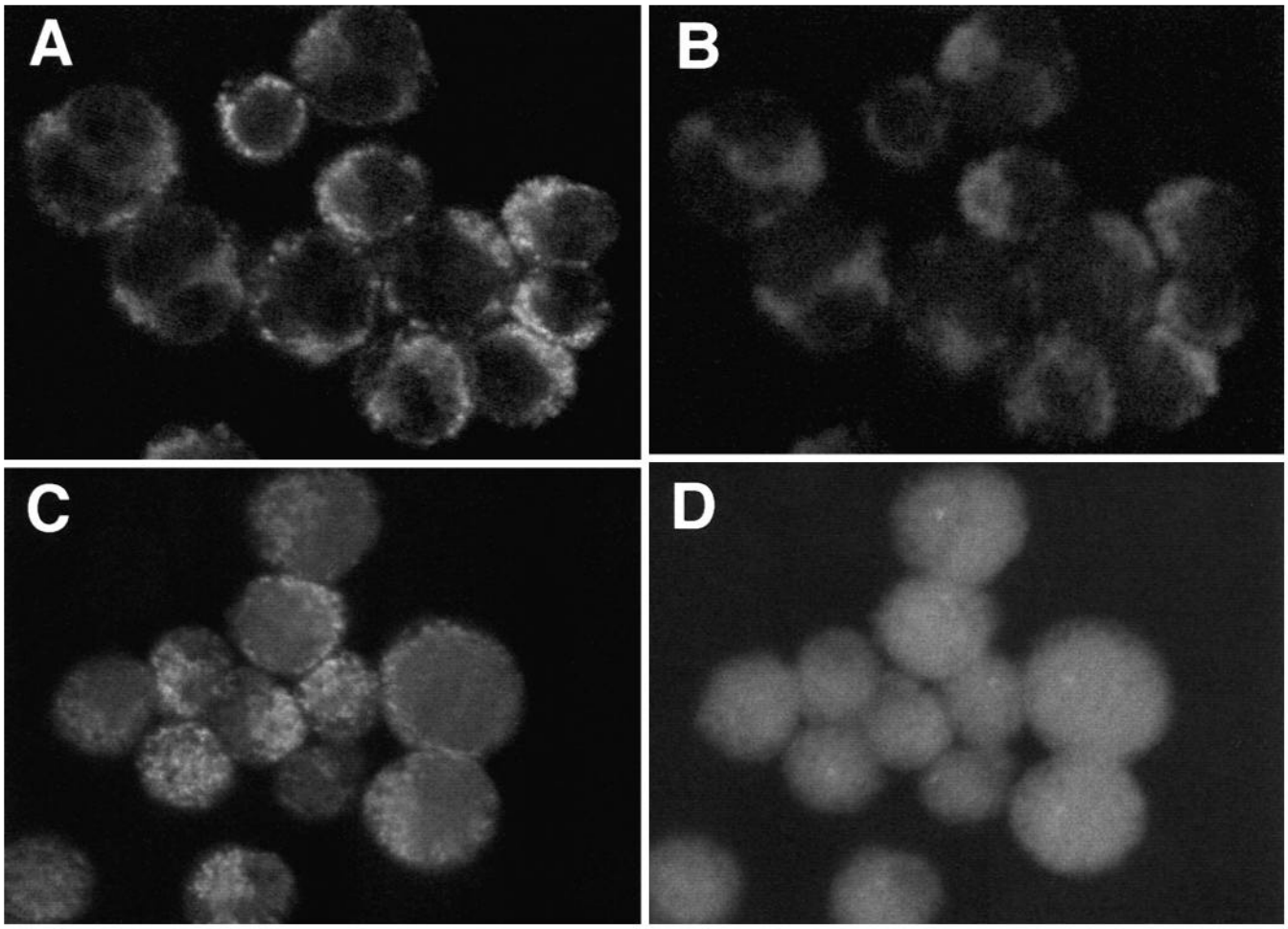

Fig. 4. Dual labeling of FL5.12 cells with FLAG-Bcl-x_L and Mitotracker. (A,B) FL5.12 cells expressing FLAG-*mbcl-x*$_L$ were double-labeled with Mitotracker, a rhodamine dye that targets to the mitochodria and fluorescein-labeled FLAG-Bcl-x_L. (C,D) FL5.12 cells expressing FLAG-*mbcl-x*$_L$ were double-labeled with CellTracker, a rhodamine dye that accumulates in the cytosol, and fluorescein-labeled FLAG-Bcl-x_L. Confocal images of the cells stained with fluorescein-labeled FLAG-Bcl-x_L are shown in A and C. Images of the same cells stained with Mitotracker are shown in B and those stained with CellTracker in D.

both Bcl-2 and Bcl-x_L proteins (Fig. 8B). Thus, both *bcl-2β* and *bcl-x*$_β$ mRNAs are generated by unspliced events of the primary mRNA transcript and their products are largely encoded by the first coding exon of *bcl-2* and *bcl-x*.

DISCUSSION

In this report we have characterized the murine *bcl-x* gene to determine if *bcl-x* could be playing a role in the regulation of PCD during development and organogenesis. Our studies have shown that within murine tissues, *bcl-x* mRNA is expressed at various levels in most or all tissues during embryonic and postnatal development. In the adult, *bcl-x* was strikingly abundant in the brain, thymus, bone marrow and kidney. The highly regulated pattern of expression of *bcl-x* is in contrast to that observed for *bcl-2*, which is expressed at similar levels in all tissues (Negrini et al., 1987; Eguchi et al., 1992; Boise et al., 1993). We find that *bcl-x*$_L$ is the predominant *bcl-x* mRNA expressed in mouse organs. Importantly, the levels of *bcl-x*$_L$ mRNA were higher than those detected for *bcl-2* in all tissues evaluated except in lymph nodes. Furthermore, murine *bcl-x*$_L$ can prevent cell death upon growth factor withdrawal at least as well as *bcl-2*, suggesting that *bcl-x*$_L$ may play an important role in regulating cell death during development. Although definitive assessment of the function of *bcl-x*$_L$ as compared with *bcl-2* must await functional studies and quantitative evaluation of both genes at the protein level, the high level expression of *bcl-x*$_L$ in certain tissues such as brain is particularly significant. For example, recent studies have shown that the levels of Bcl-2 protein are greatly reduced or undetectable in neurons of the central nervous system (CNS) in adult mice, rhesus monkeys and humans (Merry et al., 1994). Therefore, *bcl-x*$_L$ expression may be critical for maintenance of neuronal survival in the adult CNS. The expression of *bcl-x*$_L$ in embryonic and adult tissues offers a plausible explanation to account for the normal embryonic development of mice with targeted disruption of the *bcl-2* gene (Veis et al., 1993). Similarly, in *bcl-2* deficient mice, there is normal maturation of lymphoid precursors in the thymus and bone marrow (Veis

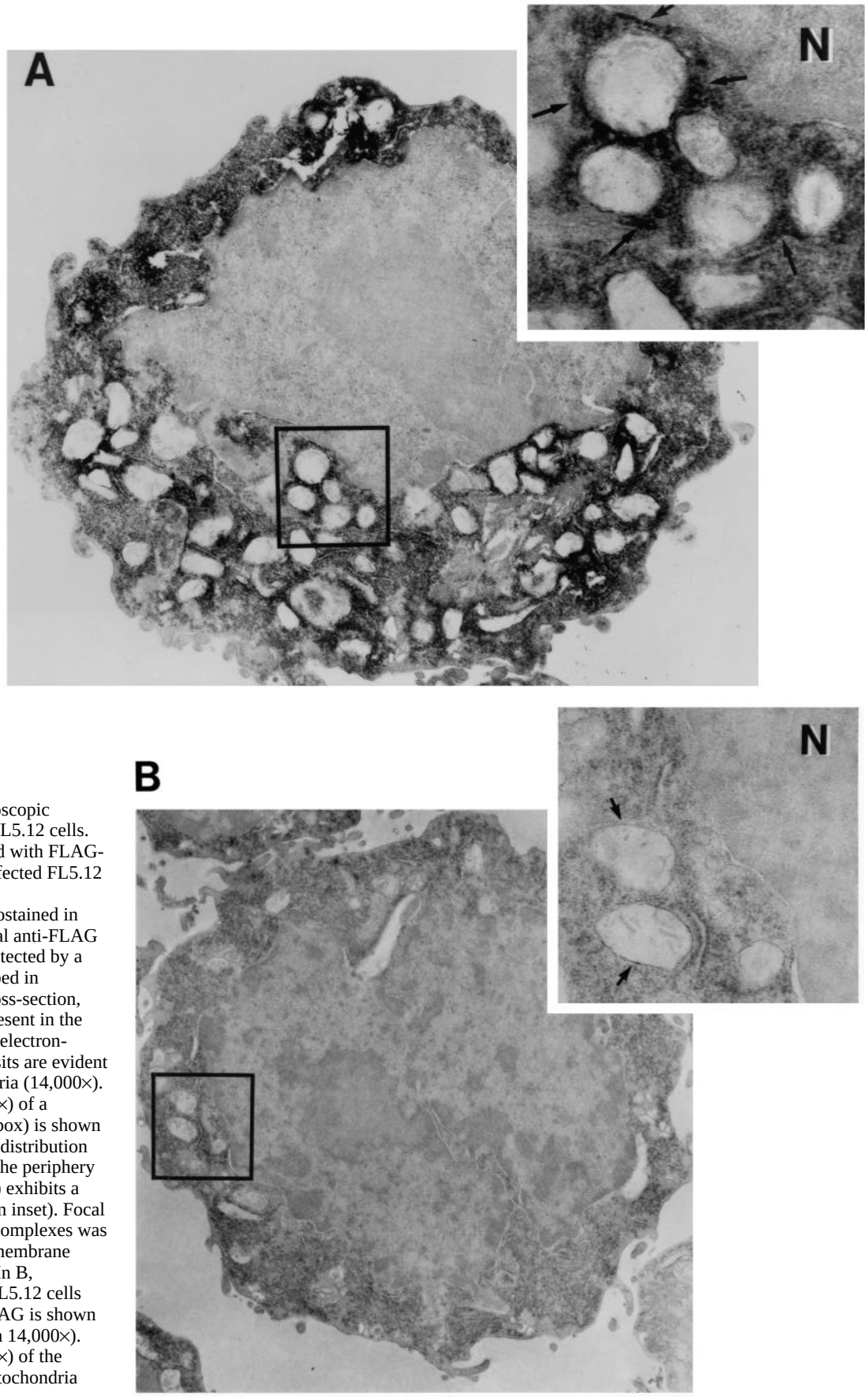

Fig. 5. Immunoelectron microscopic analysis of FLAG-Bcl-x_L in FL5.12 cells. FL5.12 cells stably transfected with FLAG-*bcl-x*$_L$ (A) or parental untransfected FL5.12 cells (B) were fixed with 2% paraformadehyde and immunostained in suspension using a monoclonal anti-FLAG antibody. The reaction was detected by a HRP-DAB reaction as described in Materials and Methods. In cross-section, abundant mitochondria are present in the cytosol. In A, the presence of electron-dense immune complex deposits are evident in the periphery of mitochondria (14,000×). Higher magnification (42,000×) of a random region of the cell (in box) is shown in the upper right corner. The distribution of electron-dense deposits in the periphery of mitochondria (long arrows) exhibits a patchy non-uniform pattern (in inset). Focal deposition of electron-dense complexes was also observed in perinuclear membrane (short arrow on top of inset). In B, immunostaining of parental FL5.12 cells using the monoclonal anti-FLAG is shown for comparison (magnification 14,000×). Higher magnification (42,000×) of the boxed area depicts several mitochondria indicated by arrows (in inset).

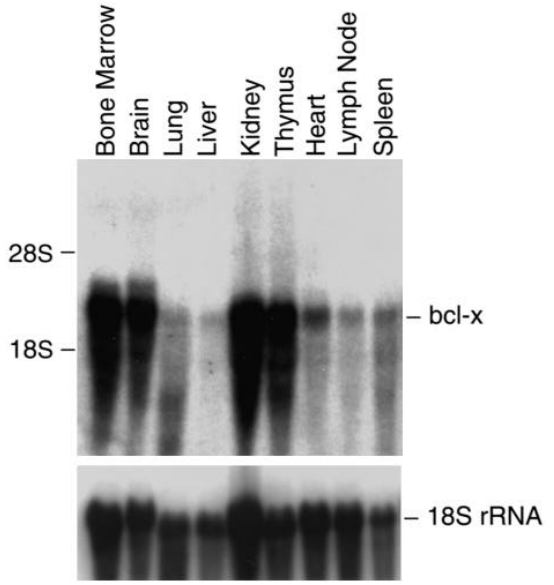

Fig. 6. Northern blot analysis of *bcl-x* mRNA in tissues from adult mice. Samples of total mRNA (12 μg) were loaded in each lane. Hybridization was performed using a 725 bp cDNA fragment containing the *bcl-x*$_L$ coding region. In all tissues examined, an approx. 3 kb band was present. As a control to evaluate the amount of mRNA loaded in each lane, the same blot was stripped and hybridized with a murine 18S rRNA probe.

et al., 1993; Nakayama et al., 1993) which may reflect the use of *bcl-x*$_L$ as a survival signal by lymphocytes to complete their differentiation into mature lymphoid cells. The disappearance of lymphoid cells in adult *bcl-2*-deficient mice (Veis et al., 1993; Nakayama et al., 1993) is consistent with the high expression of *bcl-2* in peripheral lymphoid organs such as the spleen and lymph nodes where the levels of *bcl-x*$_L$ are reduced relative to central lymphoid organs.

In the human, two mRNA forms, *bcl-x*$_L$ and *bcl-x*$_S$ were identified by cDNA cloning and PCR analysis (Boise et al., 1993). Expression of *bcl-x*$_S$ inhibited the ability of *bcl-2* to promote cell survival as determined by gene transfer experiments in growth-factor dependent cells (Boise et al., 1993). Although, *bcl-x*$_S$ functioned as a dominant negative regulator of PCD, its expression and role in modulating developmental

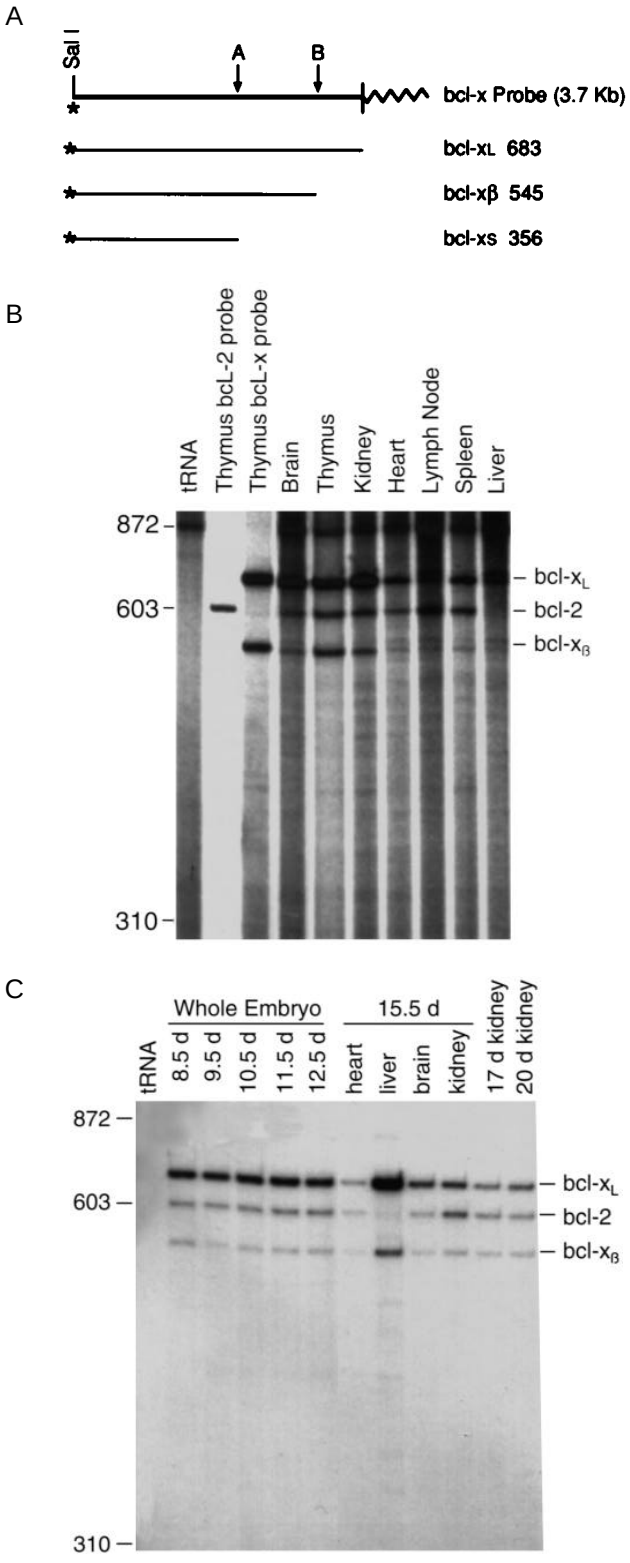

Fig. 7. Expression of *bcl-2* and *bcl-x* mRNA forms in embryonic and adult mouse tissues. (A) S1-nuclease probe constructed to detect *bcl-x* mRNA forms. The antisense strand of the *bcl-x* fragment was end-labeled at the *Sal*I site located in the coding region of the murine *bcl-x* cDNA. The region corresponding to the 5′ splice donor site used in the generation of *bcl-x*$_S$ mRNA in the human (Boise et al., 1993) is indicated by the A arrow. The exon/intron boundary in the *bcl-x*$_L$ cDNA is indicated by the B arrow. pBluescript sequences are indicated by a wavy line. Expected sizes of protected fragments for *bcl-x*$_L$, *bcl-x*$_S$ and *bcl-x*$_\beta$ mRNA forms are indicated in nucleotides. (B,C) End-labeled *bcl-2* and *bcl-x* S1-nuclease probes were simultaneously hybridized to total mRNA samples (10 μg in adult tissues, 10 μg in whole embryo samples and 5 μg in 15.5- to 20-day embryonic tissues). Both probes were labeled at a single nucleotide to allow comparison between the relative amounts of *bcl-2* and *bcl-x* mRNAs. Hybridization of both probes with a control tRNA sample is shown for comparison. Hybridization of thymus mRNA to the *bcl-2* or *bcl-x* probe alone is also shown. Notice that the *bcl-2* probe protected a fragment of 600 nucleotides (Cuende et al., 1993), whereas the *bcl-x* probe revealed protected size fragments of 683 (*bcl-x*$_L$) and 545 (*bcl-x*$_\beta$) nucleotides. An expected fragment of 356 nucleotides corresponding to the *bcl-x*$_S$ form was not detected (even at longer exposures) in any of the tissues evaluated. Size markers are in nucleotides.

processes remained unclear. Our analysis has revealed that in the mouse, *bcl-x*$_S$ is undetectable by S1-nuclease assay and PCR analysis in embryonal and adult tissues. The analysis was performed on embryonal tissues from day 8.5 to 15.5 of development, when there is extensive reshaping of tissues by PCD (Glucksmann, 1951; Hinchliffe, 1981). These findings clearly argue against a role of *bcl-x*$_S$ in modulating physiological cell death in the mouse. However, we cannot rule out that a small population of cells expresses *bcl-x*$_s$ but its level in the whole organ is too low to be detectable by current methodology. In addition, *bcl-x*$_s$ may be expressed in cell lines or upregulated during cellular activation as reported in the human system (Boise et al., 1993). We find that *bcl-x*$_L$ is the dominant *bcl-x* form in human tissues as assessed by S1-nuclease analysis (D. Grillot and G. Núñez, unpublished data) and RNase protection (L. Boise and C. Thompson, unpublished data). However, we have detected *bcl-x*$_s$ mRNA in unstimulated human thymocytes by S1-nuclease analysis confirming previous work performed by PCR (Boise et al., 1993). The molecular basis for the difference in *bcl-x*$_s$ expression between mouse and human is unclear. The *bcl-x*$_s$ mRNA species is generated by alternative use of a 5′ splice site within the first coding exon of the *bcl-x* gene (Boise et al., 1993). Comparison between the human and murine DNA sequences revealed complete conservation of the splice donor sequences in both species. Therefore, other factors such as differences within the flanking sequences to the donor/acceptor splice sites may be involved. Initial analysis revealed that the 5′ splice site of human *bcl-x* can splice to an heterologous 3′ acceptor site in mouse cells indicating that murine cells have the machinery to utilize the 5′ splice site of human *bcl-x* (D. Grillot and G. Núñez, unpublished data). An unexpected finding was the identification of an alternative mRNA species of *bcl-x*, *bcl-xβ* in mouse tissues. Our studies have shown that *bcl-xβ* is the result of an unspliced *bcl-x* mRNA transcript. The sequence of Bcl-xβ predicts that it is an intracellular soluble protein since it lacks the putative membrane-spanning region at the C terminus present in Bcl-2$_\alpha$ and Bcl-x$_L$ proteins. Because Bcl-xβ contains the 63 amino acid domain, which is critical for Bcl-x$_L$'s ability to block cell death, it is possible that Bcl-xβ may function in certain tissues such as the thymus where it is highly expressed. A similar Bcl-2 protein lacking the hydrophobic membrane-spanning domain appears capable of at least partially inhibiting apoptosis (Hockenbery et al., 1993). Clearly, further work is needed to assess the expression of the Bcl-xβ protein and its capacity to modulate apoptotic cell death.

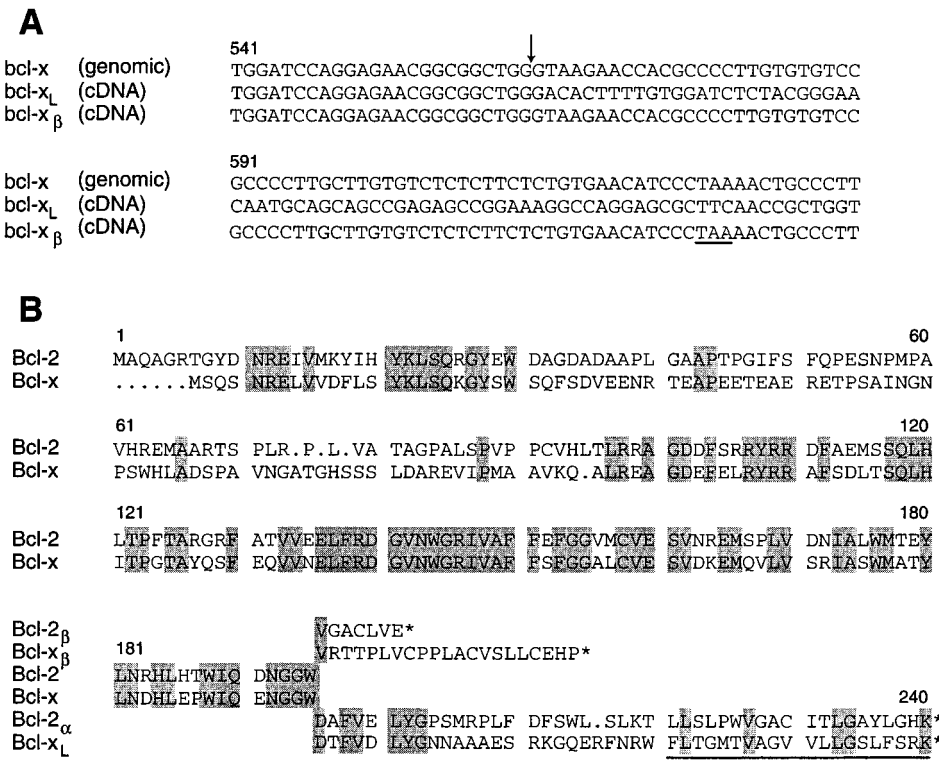

Fig. 8. Alignment between genomic *bcl-x*, *bcl-x* cDNAs, and predicted Bcl-x$_L$, Bcl-xβ and Bcl-2 proteins. (A) Genomic nucleotide sequences were obtained from a *bcl-x* genomic clone. The genomic sequence is colinear with that of the *bcl-xβ* cDNA. The donor splice site in the genomic sequence is indicated by an arrow. The predicted stop codon for the Bcl-xβ protein is underlined. (B) Alignment between Bcl-2 and predicted Bcl-x$_L$ and Bcl-xβ proteins. Bcl-2 sequences were obtained from Negrini et al., 1987. The alignment was maximized by introducing insertions marked by dots.

The mechanism by which Bcl-2 and Bcl-x$_L$ block apoptosis is unclear. Recent studies, however, have shown that Bcl-2 may function in an anti-oxidant pathway (Hockenbery et al., 1993; Kane et al., 1993). In addition, other studies have suggested that Bcl-2 may inhibit cell death by modulating Ca^{2+} fluxes across membranes of intracellular organelles (Baffy et al., 1993). The localization of Bcl-x$_L$ to the the periphery of the mitochondria and perinuclear membrane, sites where Bcl-2 also localizes (Monaghan et al., 1992; Jacobson et al., 1993; Krajewski et al., 1993), strongly suggests that both Bcl-2 and Bcl-x$_L$ proteins function in a similar manner to prevent cell death.

The authors thank Bruce Donohoe and Robin Kunkel for expert assistance with electron microscopy, Christine Viguie, Tom Komorowski and Brian Athey for advise and assistance with confocal microscopy, Justin Laby for help with confocal imaging analysis, Joseph Ruiz and Larry Holzman for RNA samples, Sue O'Shea for embryonal tissue and expert advise and Ramón Merino, Didier Grillot, Phil Simonian, and Mary Benedict for critical review of the manuscript. This work was supported by grants from the US Public Health (UM-MAC P60-AR20557), American Cancer Society, The Council for Tobacco Research-USA, and the Sandoz Foundation for Gerontological Research to G. N. M. G.-G. was supported in part by a fellowship from the North Atlantic Treaty Organization. L. H. B. is a fellow of the Leukemia Society of America. C. B. T. is supported by the Howard Hughes Medical Institute.

REFERENCES

Baffy, G., Miyashita, T., Williamson, J.R. and Reed, J.C.(1993). Apoptosis induced by withdrawal of interleukin-3 (IL-3) from an IL-3-dependent hematopoietic cell line is associated with repartitioning of intracellular calcium and is blocked by enforced Bcl-2 oncoproteinproduction. *J. Biol. Chem.* **268**, 6511-6519.

Baughman, G., Harrigan, M.T., Campbell, N.F., Nurrish, S.J. and Bourgeois, S. (1991). Genes newly identified as regulated by glucocorticoids in murine thymocytes. *Molec. Endocrinol.* **5**, 637-644.

Boise, L.H., González-García, M., Postema, C.E., Ding, L., Linsten, T., Turka, L.A., Mao, X., Núñez, G. and Thompson, C.B. (1993). bcl-x, a bcl-2-related gene that functions as a dominant regulator of apoptotic cell death. *Cell* **74**, 597-608.

Bonini, N.M., Leiserson, W.M. and Benzer, S. (1993). The eyes absent gene: genetic control of cell survival and differentiation in the developing Drosophila eye. *Cell* **72**, 379-395.

Chen-Levy, Z., Nourse, J. and Cleary, M.L. (1989). The eyes absent gene: genetic control of cell survival and differentiation in the developing Drosophila eye. *Mol. Cell. Biol.* **9**, 701-710.

Clarke, A.R., Purdie, C.A., Harrison, D.J., Morris, R.G., Bird, C.C., Hooper, M.L. and Wyllie, A.H. (1993). Thymocyte apoptosis induced by p53-dependent and independent pathways. *Nature* **362**, 849-852.

Cohen, J.J. (1991). Programmed cell death in the immune system. *Adv. Immunol.* **50**, 55-85.

Cohen, J.J. and Duke, R.C. (1984). Glucocorticoid activation of a calcium-dependent endonuclease in thymocyte nuclei leads to cell death. *J. Immunol.* **32**, 38-42.

Cuende, E., Alés-Martínez, J.E., Ding, L., González-García, M., Martínez-A. and Núñez, G. (1993). Programmed cell death by bcl-2-dependent and independent mechanisms in B lymphoma cells. *EMBO J.* **12,** 1555-1560.

Chirgwin, J.M., Przybyla, A.E., MacDonald, R.J. and Rutter, W.J. (1979). Isolation of biologically active ribonucleic acid from sources enriched in ribonuclease. *Biochemistry* **18**, 5294-5299.

Eguchi, Y., Ewert, D.L. and Tsujimoto, Y. (1992). Isolation and characterization of the chicken bcl-2 gene: expression in a variety of tissues including lymphoid and neuronal organs in adult and embryo. *Nucl. Acids Res.* **20**, 4187-4192.

Ellis, H.M. and Horvitz, H.R. (1986). Genetic control of programmed cell death in the nematode C. elegans. *Cell* **44,** 817-829.

Ellis, H.M., Yuan, J. and Horvitz, H.R. (1991). Mechanisms and functions of cell death. *Annu Rev. Cell Biol.* **7**, 663-698.

Fuhlbrigge, R.C., Fine, S.M., Unanue, E.R. and Chaplin, D.D. (1988). Expression of membrane interleukin 1 by fibroblasts transfected with murine pro-interleukin 1 alpha cDNA. *Proc. Natl Acad. Sci. USA* **85**, 5649-5653.

García, I., Martinou, I., Tsujimoto, Y. and Martinou, J.C. (1992). Prevention of programmed cell death of sympathetic neurons by the bcl-2 proto-oncogene. *Science* **258,** 302-304.

Glucksmann, A. (1951). Cell deaths in normal vertebrate ontogeny. *Biol . Rev. Cambridge Philos. Soc.* **26**, 59-86.

Hengartner, M.O., Ellis, R.E. and Horvitz, H.R. (1992). Caenorhabditis elegans gene ced-9 protects cells from programmed cell death. *Nature* **356,** 494-499.

Hinchliffe, J.R. (1981). *Cell Death in Biology and Pathology*, pp.35-78. Chapman and Hall Press, London.

Hockenbery, D.M., Núñez, G., Milliman, C., Schreiber, R.D. and Korsmeyer, S.J. (1990). Bcl-2 is an inner mitochondrial membrane protein that blocks programmed cell death. *Nature* **348**, 334-336.

Hockenbery, D.M., Oltvai, Z.N., Yin, X-M., Milliman, C.T. and Korsmeyer, S.J. (1993). Bcl-2 functions in an antioxidant pathway to prevent apoptosis. *Cell* **75**, 241-251.

Hopp, T.P., Prickett, K.S., Price, V.L., Libby, R.T., March, C.J., Cerretti D.P., Urdal, D.L. and Conlon, P.J. (1988). A short polypeptide marker sequence useful for recombinant protein identification and purification. *Bio/Technology* **6**, 1204-1210.

Ishida, V., Agata, Y., Shibahara, K. and Honjo, T. (1992). Induced expression of PD-1, a novel member of the immunoglobulin gene superfamily, upon programmed cell death. *EMBO J.* **11**, 3887-3895.

Jacobson, M.D., Burne, J.F., King M.P., Miyashita, T., Reed, J.C. and Raff, M.C. (1993). Bcl-2 blocks apoptosis in cells lacking mitochondrial DNA. *Nature* **361,** 365-369.

Kane , D.J., Sarafian, T.A., Anton, R., Hahn, H.,Gralla, E.B., Valentine, J.S., Ord, T. and Bredesen, D.E. (1993). Bcl-2 inhibition of neural death: decreased generation of reactive oxygen species. *Science* **262**, 1274-1276.

Kolodziej, P.A. and Young, R.A. (1991). Epitope tagging and protein surveillance. *Methods Enzymol* **194**, 508-519.

Kozak, M. (1987). An analysis of 5′-noncoding sequences from 699 vertebrate messenger RNAs. *Nucl. Acids Res.* **15,** 8125-8148.

Krajewski, S., Tanaka, S., Takayama, S., Schibler, M.J., Fenton, W. and Reed, J.C. (1993). Investigation of the subcellular distribution of the bcl-2 oncoprotein: residence in the nuclear envelope, endoplasmic reticulum, and outer mitochondrial membranes. *Cancer Res.* **53**, 4701-4714.

Lowe, S.W., Schmitt, E.M., Smith, S.W., Osborne, B.A. and Jacks, T. (1993). p53 is required for radiation-induced apoptosis in mouse thymocytes. *Nature* **362**, 847-849.

Martin, D.P., Schmidt, R.E., DiStefano, P.S., Lowry, O.H. Carter, J.G. and Johnson, E.M. Jr. (1988). Inhibitors of protein synthesis and RNA synthesis prevent neuronal death caused by nerve growth factor deprivation. *J. Cell Biol.* **106**, 829-844.

McCall, C.A. and Cohen, J.J. (1991). Programmed cell death in terminally differentiating keratinocytes: role of endogenous endonuclease. *J. Invest. Dermatol.*. **97**, 111-114.

Merry, D.E., Veis, D.J., Hickey, F. and Korsmeyer, S.J. (1994). bcl-2 protein expression is widespread in the developing nervous system and retained in the adult PNS. *Development* **120**, 301-311.

Miura, M., Zhu, H., Rotello, R., Hartwieg, E. A. and Yuan, J. (1993). Induction of apoptosis in fibroblasts by IL-1 beta-converting enzyme, a mammalian homolog of the C. elegans cell death gene ced-3. *Cell* **75**, 653-660.

Monaghan, P., Robertson, D., Amos, T.A.S., Dyer, M.J.S., Mason, D.Y. and Greaves, M.F. (1992). Ultrastructural localization of bcl-2 protein. *J. Histochem. Cytochem.* **40**, 1819-1825.

Nakayama, K., Nakajama, K., Negishi, I., Kuida, K., Shinkai, Y., Louie, M.C., Fields, L.E., Lucas, P.J., Stewart, V., Alt, F.W. and Loh, D.Y. (1993). Disappearance of the lymphoid system in Bcl-2 homozygous mutant chimeric mice. *Science* **261**, 1584-1588.

Negrini, M., Silini, E., Kozak, C., Tsujimoto, Y. and Croce, C.M. (1987). Molecular analysis of mbcl-2: structure and expression of the murine gene homologous to the human gene involved in follicular lymphoma. *Cell* **49**, 455-463.

Nguyen, M., Millar, D.G., Yong, V.W., Korsmeyer, S.J., and Shore, G.C. (1993). Targeting of Bcl-2 to the mitochondrial outer membrane by a COOH-terminal signal anchor sequence. *J. Biol. Chem.* **268**, 25265-25268.

Núñez, G., London, L., Hockenbery, D., Alexander, M., McKearn, J.P. and Korsmeyer, S.J. (1990). Deregulated Bcl-2 gene expression selectively prolongs survival of growth factor-deprived hemopoietic cell lines. *J. Immunol.* **144**, 3602-3610.

Oppenheim, R.W. (1991). Cell death during development of the nervous system. *Annu. Rev. Neurosci.* **14**, 453-501.

Owens, G.P., Hahn, W.E. and Cohen, J.J. (1991). Identification of mRNAs associated with programmed cell death in immature thymocytes. *Mol. Cell. Biol.* **11**, 4177-4188.

Ryan, J.J., Danish, R., Gottlieb, C.A. and Clarke, M.F. (1993). Cell cycle analysis of p53-induced cell death in murine erythroleukemia cells. *Mol. Cell. Biol.* **13**, 711-719.

Tsujimoto, Y. and Croce, C.M. (1986). Analysis of the structure, transcripts, and protein products of bcl-2, the gene involved in human follicular lymphoma. *Proc. Natl. Acad. Sci. USA* **83**, 5214-5218.

Vaux, D.L. Cory, S. and Adams, J.M. (1988). Bcl-2 gene promotes haemopoietic cell survival and cooperates with c-myc to immortalize pre-B cells. *Nature* **335**, 440-442.

Veis, D.J., Sorenson, C.M., Shutter, J.R. and Korsmeyer, S.J. (1993). Bcl-2-deficient mice demonstrate fulminant lymphoid apoptosis, polycystic kidneys, and hypopigmented hair. *Cell* **75**, 229-240.

Williams, G.T. (1991). Programmed cell death: apoptosis and oncogenesis. *Cell* **65**, 1097-1098.

Yonish-Rouach, E., Resnitzky, D., Lotem, J., Sachs, L., Kimchi, A. and Oren, M. (1991). Wild-type p53 induces apoptosis of myeloid leukaemic cells that is inhibited by interleukin-6. *Nature* **352**, 345-347.

Yuan, J. and Horvitz, H.R. (1990). The Caenorhabditis elegans genes ced-3 and ced-4 act cell autonomously to cause programmed cell death. *Dev. Biol.* **138**, 33-41.

Yuan, J., Shaham, S., Ledoux, S., Ellis, H.M. and Horvitz, H.R. (1993). The C. elegans cell death gene ced-3 encodes a protein similar to mammalian interleukin-1 beta-converting enzyme. *Cell* **75**, 641-652.

Accepted 11 July 1994

Note added in proof

Gene Bank accession numbers for DNA sequences are L35048 and L35049.